# A PLL-based Retro-Directive Antenna System for Communications with Arbitrary Frequency Gaps

Andreas Winterstein, Lukasz A. Greda, Achim Dreher
Institute of Communications and Navigation, German Aerospace Center (DLR), 82234 Wessling, Germany
{andreas.winterstein; lukasz.greda; achim.dreher}@dlr.de

***Abstract*—Retro-directive antenna systems are of special interest in satellite communications due to their self-tracking capabilities. Since frequency bands are regulated, a key issue is the realization of a large frequency gap between transmitted and received signal. In this paper, we present simulations of a novel phase-locked loop (PLL) based retro-directive antenna system for C-band which can realize arbitrary frequency translation between received and transmitted signal. It is also able to work with different array element spacings and can correct beam pointing errors. We show bistatic radiation patterns which are the response to plane waves impinging from different directions on a system with four element arrays. A frequency translation from 5.8 to 7.0 GHz is shown for different array element spacing. We demonstrate the suitability of the proposed system architecture for retro-directive applications. It can realize large frequency gaps while keeping system complexity on a reasonable level.**

***Index Terms*—Antenna arrays, phased arrays, directive antennas, antenna radiation patterns.**

## I. Introduction

Retro-directive antenna systems have been a topic of ongoing research during the last decades [1]. Applications are seen e.g. in mobile communication where moving user terminals can automatically track a stationary satellite [2]. But also terrestrial communication is a potential field of interest, where directive transmitter systems are needed as frequencies become sparse.

The appealing property of a retro-directive transceiver is that it transmits a response into the direction of an incoming signal, without performing complex digital computations [3]. The return signal is created by conjugating the phase of the received signal. A general problem is to realize a frequency gap between incoming and re-transmitted signal, as this leads to beam pointing errors [4]. However, for bidirectional communication a frequency translation is essential. Since the use of radio frequencies is subject to national and international regulation, communication systems must comply to the given standards and realize the necessary gaps between receiving and transmitting bands.

A phase-locked loop (PLL) based architecture for retro-directive systems has first been proposed in [5]. Such architectures make use of the tracking ability of PLLs in order to capture a received signal. In comparison to other solutions based on heterodyne techniques, the received signal can be extracted and the gain of the receiver (Rx) array is used when PLLs are employed which makes the system more efficient [6].

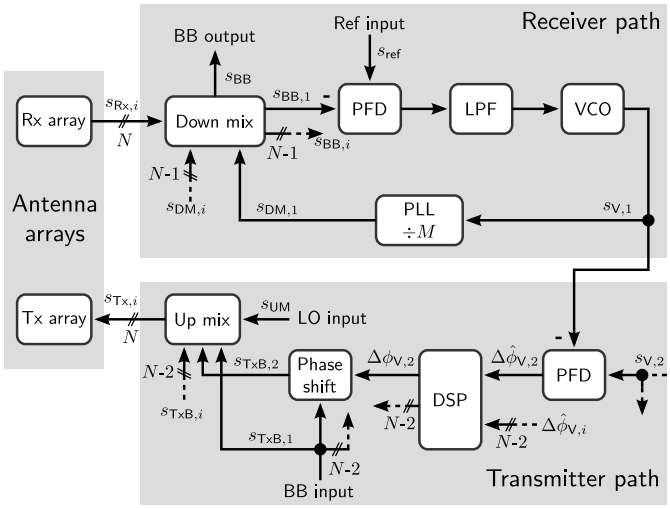


Fig. 1: Block diagram of the proposed retro-directive transceiver. Incoming signals are received by the Rx array and down mixed. The down mix signal is generated by a nested PLL structure. Phase differences between the VCO signals are used for Tx beamforming.

In this work, we propose an innovative PLL-based retro-directive antenna system that can realize arbitrary frequency gaps by separating Rx and transmitter (Tx) paths. Phase detection is performed in the Rx section. Digital signal processing (DSP) is used for calibration and to correct beam pointing errors by adjusting the Tx signal phases. To demonstrate the applicability of our system, we perform time-domain simulations for a C-band transceiver, using $4 \times 1$ patch antenna arrays. Bistatic radiation patterns are shown to verify the retro-directive behavior of the system and prove the beamforming abilities.

## II. System architecture

The proposed retro-directive transceiver is shown in Fig. 1. For better readability, only one Rx and Tx channel is shown in detail. Incoming electromagnetic waves impinge on the Rx array of the system and the response signal is sent from the Tx array. The single baseband (BB) output yields the combined received signal, thereby making use of the Rx array gain. The system has inputs for a stable reference frequency, BB input for the Tx signal, and a local oscillator (LO) input for up mix. To get classic retro-directive behavior, the BB output and input

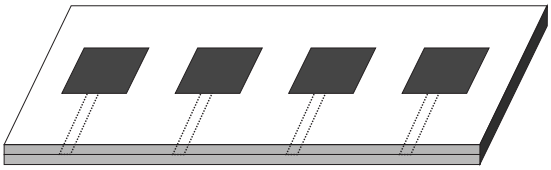

Fig. 2: Designed $4 \times 1$ microstrip patch array with proximity coupling.

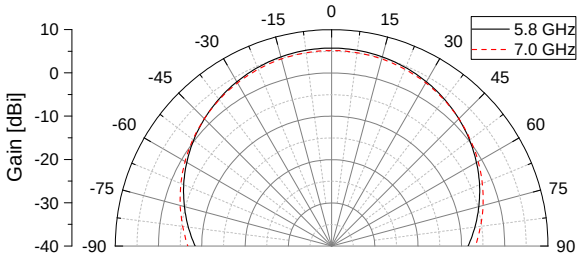


Fig. 3: Gain patterns of single patch antennas for 5.8 and 7.0 GHz.

can be connected. For a bidirectional communication, the BB input is used for the terminal Tx messages.

The receiver architecture is based on PLLs, an approach which was introduced in [5] and is also used in current implementations [2]. The proposed retro-directive antenna system is implemented in C-band. This band can be used for fixed satellite services, high altitude platforms, and mobile communication. The system parts and functional principle will be described in the following.

### A. Antenna arrays

To account for the influence of non–isotropic radiation patterns and mutual coupling between elements of real antenna arrays, two separate $4 \times 1$ arrays for 5.8 and 7.0 GHz are designed and simulated using commercial software CST Microwave Studio. Fig. 2 shows a sketch of the designed arrays that use square patch antennas proximity coupled to microstrip feed lines.

As antenna substrates two Rogers RT/duroid 6002 high frequency laminates with $\varepsilon_r = 2.94$ and the thickness of 1.524 mm each are used. The square patches have lengths of 12.8 and 10.2 mm for 5.8 and 7.0 GHz, respectively. The feed lines have a width of 3.6 mm for both antennas. Using the same substrate thicknesses for the both frequencies results in various electrical thickness of the antennas and therefore leads to slightly different radiation patterns. Fig. 3 shows gain patterns of single patch antennas for the both frequencies. It can be seen that due to higher electrical thickness the radiation pattern at 7.0 GHz is slightly broader than at 5.8 GHz.

The inter-element spacing for the 7.0 GHz array is one half the free wavelength (21.4 mm). Two versions of the $4 \times 1$ array for 5.8 GHz are simulated: with the same electrical spacing of one half the free wavelength (26 mm) and the same absolute spacing as for the 7.0 GHz array (21.4 mm). In the latter case mutual coupling between the antenna elements is increased.

### B. Receiver path

The received signals $s_{\mathsf{Rx},i}$ are individually down mixed and low-pass filtered, so only the lower side band remains. The mixing signals $s_{\mathsf{DM},i}$ are thereby created by nested PLL structures. It should be noted that the shown feedback loop is used for all $N$ channels but only one channel is shown in Fig. 1. All signals are assumed to be sinusoidal and of the form

$$s_x(t) = A_x \cos\left(2\pi f_x t + \phi_x\right). \tag{1}$$

Thereby, $A_x$, $f_x$, and $\phi_x$ denote the amplitude, frequency, and phase of the signal, respectively. The index $x$ is used to differentiate between the signal. It is substituted by the corresponding abbreviation, i.e. Rx, Tx, BB, etc.

The incoming down mixed signal $s_{\mathsf{BB},i}$ is fed into a phase-frequency detector (PFD) where it is compared to a reference signal. This signal must be the same for all $N$ channels. The PFD output signal is the deviation between the two inputs, i.e. an error signal. After smoothing by a low-pass filter (LPF), the error is used to steer a voltage controlled oscillator (VCO) which produces a low frequency signal $s_{\mathsf{V},i}$. A subsequent PLL with division factor $M$ synthesizes this into the down mix signal. If the PLL is locked, its output signal is

$$s_{\mathsf{DM},i} = A_{\mathsf{DM},i} \cos\left(2\pi M f_{\mathsf{V},i} t + M\phi_{\mathsf{V},i}\right). \tag{2}$$

The feedback structure ensures that the VCO signal $s_{\mathsf{V},i}$ is adjusted such that the PFD output tends to zero, i.e. all $s_{\mathsf{BB},i}$ and $s_{\mathsf{ref}}$ are phase aligned. Thus, when all $s_{\mathsf{BB},i}$ are summed, they superimpose constructively for the BB output signal and $\phi_{\mathsf{BB},i} = \phi_{\mathsf{BB}}$.

In order to phase align the BB signals, the down mix signals must be phase shifted with respect to each other. When the PLLs are in the steady state this means that

$$\phi_{\mathsf{DM},i} = \phi_{\mathsf{Rx},i} + \phi_{\mathsf{BB}}. \tag{3}$$

On reception, the system behaves like a phased array, thus making use of the array gain.

### C. Transmit signal generation

The transmitter path shown in Fig. 1 generates a return signal and uses beamforming to send it towards the incoming signal direction. At the BB input, the low frequency return signal is connected. It is split up into $N$ branches of which $N-1$ are individually phase shifted. Finally, all signals are mixed up to the transmit frequency, using an LO input, and are fed to the Tx array.

A set of PFDs determines the phase differences between adjacent $s_{\mathsf{V},i}$. It follows from (2) and (3) that the difference signals after this stage for $i \in 2, \ldots, N$ are

$$\Delta\hat{\phi}_{\mathsf{V},i} = a\left(\frac{\phi_{\mathsf{Rx},i} - \phi_{\mathsf{Rx},i-1}}{M} + \frac{2\pi n}{M}\right), \tag{4}$$

where $a$ is a proportionality constant which depends on the PFD implementation and $M$ is the division factor of the

PLLs in the receiver path. The second term describes phase ambiguities introduced by the mapping of the Rx phase differences onto VCO signals. That means, Rx phases have a periodicity of $2\pi/M$ within $\Delta\hat{\phi}_{\mathsf{V},i}$. a DSP unit is used in order to get rid of these ambiguities and create steering signals for the subsequent phase shifters.

Since the Tx beam shall point towards the direction of reception, the obtained phase differences must be conjugated and adapted to the phase shifter sensitivity $S$. The DSP block output is therefore of the form

$$\Delta\phi_{\mathsf{V},i} = \frac{1}{S}\frac{d_{\mathsf{Tx}}}{\lambda_{\mathsf{Tx}}}\frac{\lambda_{\mathsf{Rx}}}{d_{\mathsf{Rx}}}\left(\phi_{\mathsf{Rx},i-1} - \phi_{\mathsf{Rx},i}\right), \tag{5}$$

where $d_x$ is the element spacing for the respective array, while $\lambda_x$ is the free-space wavelength for the respective frequency. It should be noted that non-linear phase shifter behavior can also be equalized by the DSP although not regarded here.

Tx pointing errors, so called array squint [4], are a problem for retro-directive systems which perform frequency translation but have the same element spacing $d_x$ for both arrays. By separating transmit signal generation from the receiver path, the proposed system architecture can correct such errors and is therefore able to work with arbitrary frequencies and element spacings.

### D. Realization challenges

Up to the present time, the proposed system architecture is not realized as an experimental setup. We are aware of the challenge that the transition from simulation to a working demonstration system poses. In the Rx section, stability plays an important role. The feedback structure has to be carefully designed in order to reach stable operation conditions, within a reasonable amount ot time. The PLL division factor $M$ depends on $f_{\mathsf{rx}}$ and $f_{\mathsf{ref}}$. However as can be seen from (4), it strongly influences the level of the PFD output and therefore phase detection accuracy. Especially for high $f_{\mathsf{Rx}}$, it may be necessary to mix down the Rx signals in two stages to keep $M$ small.

An important part is the design for the up and down mix signal paths. For the simulation, the accuracy of Rx phase detection and Tx beamforming relies on the assumption that the $s_{\mathsf{DM},i}$ and $s_{\mathsf{UM},i}$ arrive with equal phases at the mixers. The same is true for the connections to the antenna arrays. In the real system such ideal behavior can not be assumed. However, the system architecture performs correct Rx beamforming automatically. Deviations in phase detection and Tx beamforming must be equalized by the DSP block. This means that careful calibration of the system is necessary. An implementation of the proposed architecture should have a possibility to perform this calibration online.

Regarding the DSP block, one should consider that the output of the PFDs will change rather slowly in the steady state. Therefore a cheap field-programmable gate array (FPGA) or even a microcontroller with slow analog-to-digital conversion is sufficient for the task. The different $\Delta\hat{\phi}_{\mathsf{V}i}$ can even be sampled serially employing a multiplexer. Thus the complexity of the DSP part of the architecture is far beyond that of a digital smart antenna system.

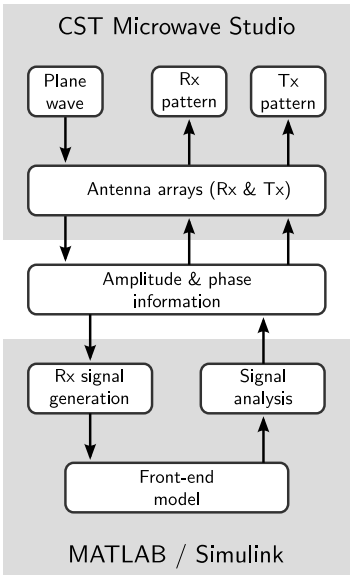


Fig. 4: Overview of the time-domain simulation chain. *CST Microwave Studio* is used for electromagnetic simulations while *MATLAB* and *Simulink* contribute results for system and signal-related parts.

## III. Time-domain simulation method

The proposed retro-directive antenna system is analyzed by time-domain simulation. Fig. 4 shows the utilized tools: *CST Microwave Studio* is used to simulate the antenna arrays. Planar waves are generated and received by the Rx array. The resulting amplitude and phase information at the individual antenna ports is stored and used to create the *CST* reception pattern.

From the stored information, we create input signals for the *Simulink* front-end model. This model comprises the receiver and transmitter paths from Fig. 1. Simulation time must be chosen such that the PLLs reach their steady state. The generated down mix and Tx signals are analyzed in *MATLAB* and their amplitude and phase information is extracted and stored.

From this we generate excitation signals at the ports of the *CST* antenna models. The result are bistatic radiation patterns including the Rx and Tx beamforming produced by the front-end.

The proposed method enables us to link an electromagnetic simulation tool with the model of the front-end. The *Simulink* model comprises the system parts shown in Fig. 1 down to the component level. Thus we are able to parameterize the subsystems accurately and analyze their behavior in detail. This is an advantage when building an experimental setup with commercially available components as their specifications can be considered and simulated before prototyping.

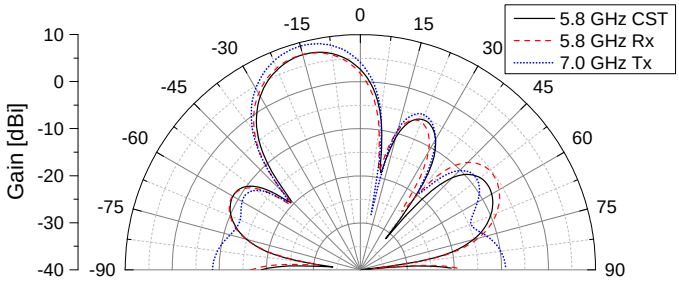


(a) Incident wave from $-15°$

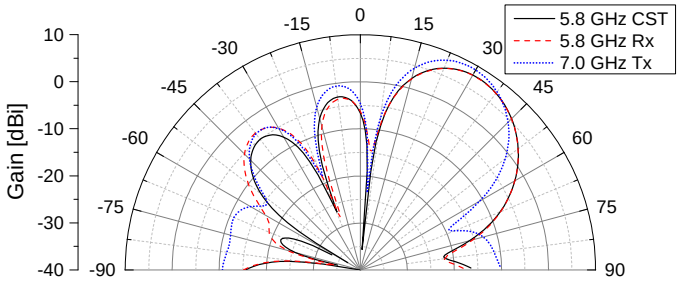


(b) Incident wave from $30°$

Fig. 5: Bistatic patterns with both arrays having half-wavelength element spacing, i.e. $d_{\mathsf{Rx}}/\lambda_{\mathsf{Rx}} = d_{\mathsf{Tx}}/\lambda_{\mathsf{Tx}} = 0.5$. Solid curve: Rx pattern from EM simulation. Dashed curve: Rx beamforming. Dotted curve: Tx beamforming.

TABLE I: Simulated radiation patterns for $d_{\mathsf{Rx}}/\lambda_{\mathsf{Rx}} = 0.5$ and different plane wave angles-of-arrival (AoA).

| AoA [°] | | dir. [°] | Main lobe gain [dBi] | width [°] | Side lobe level [dB] |
|---|---|---|---|---|---|
| $-15$ | CST | $-14.0$ | 7.31 | 24.2 | $-12.7$ |
| | Rx | $-15.0$ | 7.37 | 24.2 | $-12.7$ |
| | Tx | $-15.0$ | 9.22 | 23.8 | $-13.6$ |
| 30 | CST | 31.0 | 7.82 | 27.8 | $-10.7$ |
| | Rx | 32.0 | 7.79 | 27.7 | $-11.1$ |
| | Tx | 29.0 | 9.07 | 24.3 | $-9.7$ |

## IV. Results

Simulations are performed with plane waves incident from $-15°$ and $30°$. For the front-end, the simulated time span was always $0.5\,\mu$s. This ensures that all beamforming coefficients are stable. It can be expected, that steady values are reached in an even shorter time but this requires tuning of numerous parameters in the model and is beyond the scope of this work.

The bistatic radiation patterns for the two array configurations are shown in Figs. 5 and 6. The black, solid curves denote the receiving pattern simulated by *CST* when the array is excited by a plane wave from the given direction. The red, dashed curves show the Rx beamforming which is achieved in the front-end by multiplication of the incoming signal with phase shifted down mix signals. Finally, the blue, dotted curves show the Tx beamforming. This is the result of the phase shifted signals created in the Tx path.

Regarding the results for the half-wavelength configuration in Fig. 5, the retro-directive performance of the system is

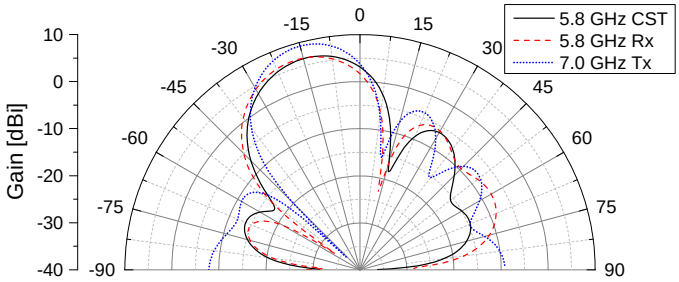


(a) Incident wave from $-15°$

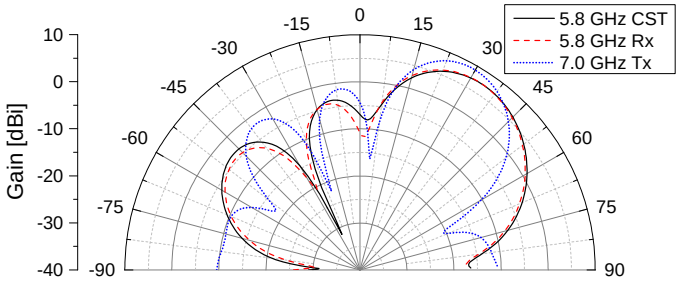


(b) Incident wave from $30°$

Fig. 6: Bistatic patterns with both arrays having equal element spacing, i.e. $d_{\mathsf{Rx}}/\lambda_{\mathsf{Rx}} = 0.414$ and $d_{\mathsf{Tx}}/\lambda_{\mathsf{Tx}} = 0.5$.

TABLE II: Simulated radiation patterns for $d_{\mathsf{Rx}}/\lambda_{\mathsf{Rx}} = 0.414$ and different plane wave angles-of-arrival (AoA).

| AoA [°] | | dir. [°] | Main lobe gain [dBi] | width [°] | Side lobe level [dB] |
|---|---|---|---|---|---|
| $-15$ | CST | $-15.0$ | 6.44 | 28.7 | $-12.8$ |
| | Rx | $-17.0$ | 6.62 | 28.3 | $-12.4$ |
| | Tx | $-15.0$ | 9.22 | 23.7 | $-13.1$ |
| 30 | CST | 32.0 | 7.23 | 32.3 | $-11.3$ |
| | Rx | 33.0 | 7.27 | 32.5 | $-11.4$ |
| | Tx | 29.0 | 9.05 | 24.4 | $-10.4$ |

evident: The Rx beam is steered towards the incoming wave and matches the result from *CST* very well. The outgoing Tx beam is also clearly directed towards the received wave. Side lobe levels are increasing for higher steering angles, as can be expected. The similarity between Rx and Tx patterns is due to $d/\lambda$ being $0.5$ in both cases. Key values of the generated beams are listed in Table I. This data was extracted from the *CST* simulation and it confirms the similarity between the patterns.

If we take a look at Fig. 6, it is clear that also here retro-directive action is performed for the two incident angles. Due to closer element spacing, the Rx pattern is less directive than in Fig. 5, but its side lobe levels are lower instead. The position of gain minimums is not the same for Rx and Tx patterns because of the different $d/\lambda$. Important pattern characteristics are listed in Table II.

## V. Conclusion

In this paper we have proposed a novel retro-directive architecture using a PLL-based receiver. The system employs the gain of the Rx array on reception, i.e. automatically

steers a beam towards the incident wave. Beamforming for re-transmission is achieved by phase shifting the Tx signals according to the phase information extracted by the Rx path. A small DSP block enables us to correct array squint effects due to frequency translation or different array topologies. Thus arbitrary frequency gaps between Rx and Tx can be realized.

We have demonstrated the retro-directive performance of the proposed system by simulation, using time-domain based tools. Results are shown for a C-band transceiver with four element line arrays at $5.8$ and $7.0\,\mathrm{GHz}$. The resulting bistatic radiation patterns show excellent retro-directive behavior.

As a next step, an experimental prototype of the system shall be built in order to validate the simulated performance. Further investigation will be done towards an enhancement of the beamforming by digital signal processing. Currently, only phased array performance is obtained. If it were possible to employ more sophisticated beamforming techniques without increasing complexity too much, this would be an essential gain in performance.

The proposed system architecture is a promising candidate for retro-directive applications. Especially the lack of power hungry, high-throughput digital components is an advantage in terms of efficiency and scalability compared to fully digital approaches.

## REFERENCES


[1] V. Fusco and N. Buchanan, "Developments in retrodirective array technology," *Microwaves, Antennas & Propagation, IET*, vol. 7, no. 2, pp. 131 – 140, January 2013.

[2] N. B. Buchanan, V. F. Fusco, M. van der Vorst, and O. Malyuskin, "A high performance circular polarised retrodirective antenna with basic array function for service activated satcom systems," in *Antennas and Propagation (EUCAP), 2012 6th European Conference on*, Prague, March 2012, pp. 2798 – 2801.

[3] R. Y. Miyamoto and T. Itoh, "Retrodirective arrays for wireless communications," *IEEE Microwave Magazine*, vol. 3, no. 1, pp. 71 – 79, March 2002.

[4] C. Y. Pon, "Retrodirective array using the heterodyne technique," *IEEE Transactions on Antennas and Propagation*, vol. 12, no. 2, pp. 176 – 180, March 1964.

[5] P. V. Brennan, "Investigation into the multipath performance of self-phased array," in *Microwaves, Antennas and Propagation, IEE Proceedings H*, vol. 136, no. 1, February 1989, pp. 47 – 52.

[6] L. Chen, T.-L. Zhang, S.-F. Liu, and X.-W. Shi, "A bidirectional dual-frequency retrodirective array for full-duplex communication applications," *IEEE Antennas and Wireless Propagation Letters*, vol. 11, pp. 771 – 774, 2012.